Abstract

Using positron emission tomography (PET) and an acute dopamine depletion challenge it is possible to estimate endogenous dopamine levels occupying dopamine $D_{2/3}$ receptors ($D_{2/3}R$) in humans *in vivo*. Our group has developed [^{11}C]-(+)-PHNO, the first agonist radiotracer with preferential *in vivo* affinity for D_3R. Thus, the use of [^{11}C]-(+)-PHNO offers the novel possibility of, i) estimating *in vivo* endogenous dopamine levels at $D_{2/3}R$ using an agonist radiotracer, and ii) estimating endogenous dopamine levels at D_3R in extrastriatal regions such as the substantia nigra, hypothalamus and ventral pallidum. Ten healthy participants underwent a [^{11}C]-(+)-PHNO PET scan under baseline conditions and another under acute endogenous dopamine depletion achieved via oral administration of alpha-methyl-para-tyrosine (AMPT) (64mg/kg). [^{11}C]-(+)-PHNO binding was sensitive to acute dopamine depletion, allowing *in vivo* estimates of endogenous dopamine in D_2R-rich regions (caudate and putamen), mixed $D_{2/3}R$-rich regions (ventral striatum and globus pallidus), and extrastriatal D_3R rich regions (hypothalamus and ventral pallidum). Dopamine depletion decreased self-reported vigor, which was correlated with the reduction of dopamine levels in the globus pallidus. [^{11}C]-(+)-PHNO is a suitable radiotracer for use in estimating endogenous dopamine levels at D_2R and D_3R in neuropsychiatric populations.

Key Words: Dopamine, D2R, D3R, PET, AMPT, [^{11}C]-(+)-PHNO

Introduction

The dopamine system has been a key molecular target in understanding the etiology and treatment of numerous neuropsychiatric disorders. Not surprisingly, it has been the most heavily investigated neurotransmitter system in the living human brain using the molecular imaging technique positron emission tomography (PET) (Banerjee and Prante, 2012). Using radiolabelled dopamine $D_{2/3}$ receptor ($D_{2/3}R$) antagonists, such as [^{11}C]-raclopride, [^{18}F]-fallypride, and [^{11}C]-FLB 457, it has been possible to quantify the availability of $D_{2/3}R$ *in vivo* in the brains of healthy persons and persons with neuropsychiatric disease (Gjedde *et al*, 2005; Newberg *et al*, 2011; Tatsch and Poepperl, 2012). Studies *in vitro* demonstrate that $D_{2/3}R$ exist in multiple affinity states for its endogenous ligand dopamine (Cumming, 2011; Seeman, 2013; van Wieringen *et al*, 2013). These states seem to affect the binding of agonist, but not antagonist, radioligands *in vitro* (Cumming, 2011; Seeman, 2013; van Wieringen *et al*, 2013). Therefore, the use of agonist radiotracers for $D_{2/3}R$ may reveal a more physiologically relevant quantification of $D_{2/3}R$ availability in the human brain, being sensitive to changes in receptor affinity.

The positron emission tomography (PET) radiotracer [^{11}C]-(+)-PHNO is the first agonist radiotracer for $D_{2/3}R$ which has preferential affinity for the D_3 receptors (Graff-Guerrero *et al*, 2010; Graff-Guerrero *et al*, 2008; Narendran *et al*, 2006; Rabiner *et al*, 2009; Wilson *et al*, 2005). This unique property of [^{11}C]-(+)-PHNO, ~20-40 fold selectivity of D_3R over D_2R (Freedman *et al*, 1994; Gallezot *et al*, 2012; Rabiner *et al*, 2009; Searle *et al*, 2010; Seeman *et al*, 1993), results in a differential contribution of D_2R and D_3R to the [^{11}C]-(+)-PHNO signal across different regions of interest (ROI). The estimated percent of the [^{11}C]-(+)-PHNO signal *in vivo* in humans attributed to D_3R across ROIs are: the substantia nigra (~100%), hypothalamus (~100%), ventral pallidum (~75%), globus pallidus (~65%), ventral striatum (~26%), and dorsal

caudate-putamen (negligible) (Graff-Guerrero *et al*, 2010; Searle *et al*, 2013; Tziortzi *et al*, 2011).

Like the antagonist radiotracer [^{11}C]-raclopride, endogenous dopamine competes with [^{11}C]-(+)-PHNO for binding to $D_{2/3}R$ at baseline (Ginovart *et al*, 2006; Shotbolt *et al*, 2012; Willeit *et al*, 2008). The amount of endogenous dopamine occupying $D_{2/3}R$ at baseline can be estimated with such radioligands by comparing the percent change in binding potential (BP_{ND}) between a baseline scan and a scan under acute dopamine depletion (Cumming *et al*, 2002; Laruelle *et al*, 1997; Verhoeff *et al*, 2001). Acute dopamine depletion is achieved in humans using alpha-methyl-para-tyrosine (AMPT), a competitive inhibitor of tyrosine hydroxylase, which is the rate-limiting enzyme of catecholamine synthesis. Using this paradigm, altered levels of striatal endogenous dopamine occupying $D_{2/3}R$ at baseline in neuropsychiatric disorders has been demonstrated (Abi-Dargham *et al*, 2000; Abi-Dargham *et al*, 2009; Bloemen *et al*, 2013; Kegeles *et al*, 2010; Martinez *et al*, 2009).

To date, endogenous dopamine levels have not been estimated in humans using an agonist radiotracer for $D_{2/3}R$, as opposed to an antagonist. The use of an agonist radiotracer, which should more closely mimic the binding of the endogenous ligand, may offer a more sensitive and functionally significant estimate of endogenous dopamine in humans. Moreover, endogenous dopamine levels have not been estimated in D_3R-rich regions in humans such as the substantia nigra, globus pallidus, ventral pallidum, and hypothalamus. The current investigation sought to validate the use of [^{11}C]-(+)-PHNO to estimate endogenous dopamine levels at D_2R and D_3R in healthy humans.

Materials and Methods

Subjects. Twenty-four healthy participants were recruited for the study. Six participants failed screening. Two participants withdrew before the first baseline PET scan. One participant withdrew during the baseline PET scan due to nausea induced by the [^{11}C]-(+)-PHNO injection. One participant was unable to complete the study due to [^{11}C]-(+)-PHNO tracer problems prior to the post AMPT PET scan. One participant withdrew prior to the post AMPT PET scan due to akathisia, and three participants withdrew during the post AMPT scan due to feelings of claustrophobia/anxiety. Ten participants (4 female; mean age=29.1±8.4) in total completed both PET scans, under the baseline and dopamine depleted condition. All participants were free of any major medical or psychiatric disorder as determined by clinical interview, the Mini-International Neuropsychiatric Interview, basic laboratory tests, and electrocardiogram. Participants were required to have a negative urine screen for drugs of abuse and/or pregnancy at inclusion and prior to each PET scan. All participants were non-smokers. The study was approved by the Research Ethics Board of the Centre for Addiction and Mental Health (CAMH), Toronto, and no objection letter was issued by Health Canada. All the participants provided written and informed consent.

Metyrosine/AMPT administration. Dopamine depletion was induced by oral administration of 64 mg of metyrosine per kilogram of body weight over 25 hours. Independent of weight, no participant was dosed above 4,500 mg. Metyrosine was administered in six equal doses at the following times: 9:00am, 12:30pm (post 3.5 hours), 5:00pm (post 8 hours), and 9:00pm (post 12 hours) on Day1, and 6:00am (post 21 hours) and 10:00am (post 25 hours) on Day2. The post AMPT PET scan was scheduled at 12pm, 28 hours after the initial metyrosine dose. For two participants, the 12pm scan was unavailable, therefore the times for the doses were

modified to reflect the 28 hour post AMPT PET scan. The subjects were under direct observation during AMPT administration and slept overnight on an inpatient unit at CAMH to ensure the AMPT dosing schedule and monitor for potential side effects. In addition, subjects were instructed to drink at least 4 L of fluids during the 2-day admission to prevent the formation of AMPT crystals in urine. Fluid intake was carefully monitored during the study to ensure compliance. Urine samples were collected at 2:00pm on Day1 and at 9:00am on Day2 to monitor AMPT crystals in urine. In addition, in order to alkalinize the urine, which increases AMPT solubility, sodium bicarbonate (1.25 g) was given orally at 10:00pm on the evening before Day1 and at 7am on Day1 of administration.

Plasma samples. Plasma levels of prolactin, homovanillic acid (HVA), and 3-methoxy-4-hydroxyphenethyleneglycol (MHPG) were collected at 9:00am (Day1, prior to AMPT administration), 2:00pm (Day1) and 12:00pm (Day2). Plasma levels of AMPT were also collected at 2:00pm (Day1) and 12:00pm (Day2). Plasma prolactin, HVA, MHPG, and AMPT were quantified as previously described (Verhoeff *et al*, 2002). The times were modified for the two participants with the alternative post PET scan times.

Rating scales. Subjects were evaluated by the research psychiatrists (SN, GR, PG, AG) for potential side effects at the following times: 9:00am (baseline), 2:00pm (post 5 hour dose), 12:00pm (post 27 hour dose), and at 3pm (post 30 hour dose) The times were modified for the two participants with the alternative post PET scan times. The presence of adverse effects such as parkinsonian symptoms, acute dystonias, and involuntary movements was monitored using the Simpson Angus Scale (SAS), Barnes Akathisia Scale (BAS), and the Abnormal Involuntary Movement Rating Scale (AIMS). To evaluate changes in energy, mood, and subjective well-

being induced by dopamine depletion, the Profile of Mood States (POMS) and the Subjective Well-Being Under Neuroleptic Treatment (SWN) scales were administered.

PET Imaging. Participants underwent two [^{11}C]-(+)-PHNO PET scans, one under baseline conditions and another at 25 hours of starting AMPT induced dopamine depletion. The radiosynthesis of [^{11}C]-(+)-PHNO and the acquisition of PET images has been described in detail elsewhere (Graff-Guerrero *et al*, 2010; Wilson *et al*, 2000; Wilson *et al*, 2005). Briefly, images were acquired using a high resolution head-dedicated PET camera system (CPS-HRRT; Siemens Molecular Imaging, USA), which measures radioactivity in 207 brain slices with a thickness of 1.2mm each. The in-plane resolution was ~2.8mm full-width at half-maximum (FWHM). Transmission scans were acquired using a ^{137}Cs ($T_{1/2}$ = 30.2 yr, E = 662 KeV) single photon point source to provide attenuation correction, and the emission data were acquired in list mode. The raw data were reconstructed by filtered-back projection. For the baseline [^{11}C]-(+)-PHNO scans, the mean radioactivity dose was 9.2(±1.2)mCi, with a specific activity of 1113.7(±328.2)mCi/µmol, and an injected mass of 2.1(±0.4)µg. For the dopamine-depleted scans, the mean radioactivity dose was 8.7(±1.5)mCi, with a specific activity of 1024.1(±299.5)mCi/µmol, and an injected mass of 2.1(±0.3)µg. There was no difference in mean radioactivity dose ($t(9)$=0.92, p=0.38), specific activity ($t(9)$=0.96, p=0.37), or mass injected ($t(9)$=-0.32, p=0.75) between the baseline and dopamine depletion scans. [^{11}C]-(+)-PHNO scanning data was acquired for 90 min post injection. Once scanning was complete, the data was re-defined into 30 frames (1–15 of 1 min duration and16–30 of 5 min duration).

Image Analysis. The region of interest (ROI)-based analysis for [^{11}C]-(+)-PHNO has been described in detail elsewhere (Graff-Guerrero *et al*, 2008; Tziortzi *et al*, 2011). Briefly, time activity curves (TACs) from ROIs were obtained from the dynamic PET images in native space

with reference to each subjects co-registered MRI image. The co-registration of each subjects MRI to PET space was done using the normalized mutual information algorithm (Studholme *et al*, 1997) as implemented in SPM2 (SPM2, Wellcome Department of Cognitive Neurology, London; http://www.fil.ion.ucl.ac.uk/spm). The TACs were analyzed using the Simplified Reference Tissue Method (SRTM) (Lammertsma and Hume, 1996), using the cerebellum as the reference region, to derive a quantitative estimate of binding: the binding potential relative to the non-displaceable compartment (BP_{ND}) as defined by the consensus nomenclature for *in vivo* imaging of reversibly binding radioligands (Innis *et al*, 2007). The basis function implementation of the SRTM (Gunn *et al*, 1997) was applied to the dynamic PET images to generate parametric voxelwise BP_{ND} maps using PMOD (v2.7, PMOD Technologies, Zurich, Switzerland). These images were spatially normalized into MNI brain space by Nearest Neighbour interpolation with a voxel size fixed in 2 x 2 x 2 mm^3 using SPM2. Regional BP_{ND} estimates were then derived from ROIs defined in MNI space. The ventral striatum and dorsal striatum (dorsal caudate, hereafter caudate and dorsal putamen, hereafter putamen) were defined according with Mawlawi et al (Mawlawi *et al*, 2001). The globus pallidus, ventral pallidum, and hypothalamus ROIs were defined according to the criteria of Tziortzi et al (Tziortzi *et al*, 2011).

Estimating endogenous dopamine levels. Our estimate of endogenous dopamine levels at $D_{2/3}R$ is based on the occupancy model, in which endogenous dopamine competes with the binding of radiotracers like [^{11}C]-(+)-PHNO for $D_{2/3}R$ at baseline (Laruelle, 2000; Laruelle *et al*, 1997; Verhoeff *et al*, 2001). It is assumed by this model that, i) baseline $D_{2/3}R$ BP_{ND} is confounded by endogenous dopamine, such that the higher the concentration of dopamine the lower the value of $D_{2/3}R$ BP_{ND} will be obtained, ii) $D_{2/3}R$ BP_{ND} under depletion more accurately reflects the true status of $D_{2/3}R$, and, iii) the fractional increase in $D_{2/3}R$ BP_{ND} after dopamine

depletion [i.e., 100*(Depletion BP_{ND} – Baseline BP_{ND})/ Baseline BP_{ND} = $\%\Delta BP_{ND}$] is linearly proportional to the baseline dopamine concentration at $D_{2/3}R$, provided the process of dopamine depletion does not change the number and affinity of the $D_{2/3}R$. Thus, the $\%\Delta BP_{ND}$, under appropriate assumptions, is considered a semiquantitative index of endogenous dopamine levels at $D_{2/3}R$ (Verhoeff *et al*, 2001).

Statistical Analysis. Statistical analyses were conducted using SPSS (v.12.0; SPSS, Chicago, Illinois) and GraphPad (v.5.0; GraphPad Software, La Jolla California). Normality of variables was determined using the D'Agostino-Pearson test. The significance level for all testes was set at $p<0.05$ (two-tailed).

Results

AMPT-Induced ΔBP_{ND}

AMPT-dopamine depletion significantly increased [^{11}C]-(+)-PHNO BP_{ND} in the caudate ($t(9)=3.36$, p=0.008), putamen ($t(9)=5.84$, p=0.0002), ventral striatum ($t(9)=10.87$, p=0.0001), and globus pallidus ($t(9)=3.79$, p=0.004) (See Figure 1a). [^{11}C]-(+)-PHNO BP_{ND} did not change in the substantia nigra after dopamine depletion ($t(9)=0.29$, p=0.78). The percent change in BP_{ND} ($\%\Delta BP_{ND}$) at $D_{2/3}R$ was ~36% in the ventral striatum, ~33% in the putamen, ~33% in the caudate, and ~11% in the globus pallidus (See Figure 2 and Supplemental Table 1). Due to poor model fitting, [^{11}C]-(+)-PHNO BP_{ND} could not be reliably estimated in the hypothalamus for one subject and in the ventral pallidum for four subjects (See Supplemental Table 2). AMPT dopamine depletion significantly increased [^{11}C]-(+)-PHNO BP_{ND} in the hypothalamus ($t(8)=4.96$, p=0.001), observing a $\%\Delta BP_{ND}$ of 68.5%. In the ventral pallidum there was a trend

for an increase in [^{11}C]-(+)-PHNO BP_{ND} after dopamine depletion (t(5)=2.32, p=0.06), observing a $\%\Delta BP_{ND}$ of 64.8% (See Figure 1b).

Plasma Results

The average plasma concentration of AMPT after 27 hours of oral administration was 24(±11)µg/mL. Based on this average plasma concentration of AMPT, the average tyrosine hydroxylase inhibition in our sample can be estimated to be ~80% (Engelman *et al*, 1968; Laruelle *et al*, 1997; Udenfriend *et al*, 1965). AMPT-dopamine depletion significantly decreased plasma levels of HVA (t(9)=3.32, p=0.009) and MHPG (t(9)=5.72, p=0.0003) compared to baseline (See Table 1). AMPT dopamine depletion significantly increased plasma levels of prolactin (t(9)=5.83, p=0.0003). Baseline levels of HVA and MHPG did not correlate with baseline [^{11}C]-(+)-PHNO BP_{ND} in any ROI. Nor did changes in HVA and MHPG levels induced by AMPT correlate with changes in [^{11}C]-(+)-PHNO $BP_{ND.}$ However, baseline levels of prolactin correlated with baseline [^{11}C]-(+)-PHNO BP_{ND} in the caudate (r=0.71, p=0.02). Changes in prolactin levels induced by AMPT correlated with changes in [^{11}C]-(+)-PHNO BP_{ND} in the caudate (r=0.76, p=0.01) and putamen (r=0.82, p=0.004).

SUV Before and After AMPT

The averaged standard uptake values (SUVs) of [^{11}C]-(+)-PHNO in each ROI before and after AMPT-dopamine depletion are presented in Supplemental Figure 1.

Self-report Measures

POMS

AMPT-dopamine depletion significantly increased self-reported fatigue (t(9)=3.50, p=0.0068), decreased vigor (t(9)=3.75, p=0.0046), and increased tension (t(9)=2.31, p=0.046). However, changes in self-reported tension did not survive false discovery rate (FDR) correction

(See Table 2). We investigated whether changes in self-reported fatigue and vigor were related to changes in [^{11}C]-(+)-PHNO BP_{ND} in our ROIs. Change in vigor scores were negatively correlated with change in [^{11}C]-(+)-PHNO BP_{ND} in the globus pallidus (r=-0.77, p=0.009) (See Figure 3).

SWN

AMPT-dopamine depletion significantly decreased self-reported physical functioning (t(9)=3.28, p=0.009), negative sum scores (t(9)=3.22, p=0.01), and emotion regulation (t(9)=2.26, p=0.049). However, only changes in negative sum scores survived FDR correction (See Table 2). Change in negative sum scores were not correlated with change in [^{11}C]-(+)-PHNO BP_{ND} in any ROI.

Presence of Adverse Events

There was a trend for significant change in total scores on the SAS (t(9)=2.25, p=0.05), but no change in the sum of global clinical scores on the BAS (t(9)=1.00, p=0.34), as assessed from baseline to 30 hours post AMPT-dopamine depletion. There was also no change in a total score of zero on the AIMS. However, like previous dopamine depletion studies, it was clinically observed that subjects experienced strong AMPT side-effects. This is indicated by our 4 participant withdrawals prior to the post AMPT PET scan (1 due to severe akathisia and 3 due to feelings of claustrophobia/anxiety). Notably, subject #4 and #5 presented with clinically notable akathisia and all subjects reported fatigue (for a list of all subjects and their BP_{ND} data, see Supplemental Table 2). Perhaps these observations were not captured by our scales due to the timing of when these scales were administered throughout the study. Urine testing revealed that subject #8 developed a significant level of crystalluria given AMPT-dopamine depletion, and was treated after the post PET scan accordingly.

Discussion

The present investigation is the first to estimate endogenous dopamine levels at $D_{2/3}R$ using an agonist radiotracer: [^{11}C]-(+)-PHNO. Hypothetically, an agonist radiotracer for $D_{2/3}R$ should be more sensitive to changes in endogenous dopamine levels than an antagonist radiotracer. Notably, the change in striatal BP_{ND} of [^{11}C]-(+)-PHNO after dopamine depletion reported here (~30%) is much greater than has been previously reported in healthy controls using the antagonist radiotracer [^{11}C]-raclopride (~5.7-18.3%) (Kegeles *et al*, 2010; Martinez *et al*, 2009; Verhoeff *et al*, 2003; Verhoeff *et al*, 2002; Verhoeff *et al*, 2001). This may be due to [^{11}C]-(+)-PHNO being more sensitive than [^{11}C]-raclopride to changes in endogenous dopamine levels. This is consistent with the finding that an amphetamine challenge in healthy controls displaced the BP_{ND} of [^{11}C]-(+)-PHNO greater than [^{11}C]-raclopride (Shotbolt *et al*, 2012; Willeit *et al*, 2008). However, it is worth noting that while this increased sensitivity to endogenous dopamine has been demonstrated *in vivo* in humans, rodents (Kiss *et al*, 2011), and cats (Ginovart *et al*, 2006), this finding is not ubiquitous across studies (Galineau *et al*, 2006; McCormick *et al*, 2011). Furthermore, there are differences in the amount of AMPT administered across studies. However, in our sample we achieved a similar average plasma concentration of AMPT, and likely tyrosine hydroxylase inhibition, as previous studies (Kegeles *et al*, 2010; Martinez *et al*, 2009; Verhoeff *et al*, 2003; Verhoeff *et al*, 2002; Verhoeff *et al*, 2001). Finally, we cannot rule out that differences in reported dopamine estimation may be explained by differences in PET camera resolution. Directly comparing the change in [^{11}C]-(+)-PHNO and [^{11}C]-raclopride BP_{ND} after dopamine depletion in the same persons using a high-resolution PET camera is warranted.

The preferential affinity of [^{11}C]-(+)-PHNO for D_3R over D_2R affords the current investigation the ability to estimate, for the first time *in vivo* in humans, endogenous dopamine

levels at D_3R in select extrastriatal regions. The SN, GP, hypothalamus, and VP constitute those ROIs for which the majority of the [^{11}C]-(+)-PHNO BP_{ND} signal is due to D_3R binding. In the substantia nigra we did not observe a significant change in [^{11}C]-(+)-PHNO BP_{ND} after dopamine depletion. Thus, our findings suggest that acute dopamine depletion with AMPT does not alter dopamine levels in the SN (see Supplemental Text for discussion).

The magnitude of $\%\Delta BP_{ND}$ varied across ROIs. Differences in the concentrations of dopamine in these regions may explain some of the observed difference in the $\%\Delta BP_{ND}$. Investigations in rodent brains and post mortem human brains generally support that the regional concentrations of dopamine are: VS > Putamen > or = Caudate > GP > Hypothalamus > SN (Adolfsson *et al*, 1979; Versteeg *et al*, 1976). In our current investigation, the magnitude of $\%\Delta BP_{ND}$ generally followed this difference in regional dopamine concentration: VS > Putamen = Caudate > GP > SN. It has been suggested that the dopamine concentration in the human GP is one third of that in the striatum (Adolfsson *et al*, 1979). Notably, the magnitude of $\%\Delta BP_{ND}$ between the GP and striatal ROIs differed by one third. Finally, our observation of a ~33-36% ΔBP_{ND} in the striatum ROIs is in accordance with the 34% change in specific binding seen with [^{11}C]-(+)-PHNO in rodent striata after dopamine depletion with AMPT and reserpine *ex vivo* (Wilson *et al*, 2005).

However, differences in regional concentrations in dopamine cannot explain the large $\%\Delta BP_{ND}$ observed in the hypothalamus. We do not think this observation can be easily explained by the greater affinity of [^{11}C]-(+)-PHNO for D_3R over D_2R, since the $\%\Delta BP_{ND}$ varied across all the D_3R-rich regions. Likewise, any potential non-tracer conditions at D_3R cannot readily explain the large magnitude of $\%\Delta BP_{ND}$ observed in the hypothalamus and ventral pallidum, especially

since such conditions should reduce changes in BP_{ND} due to dopamine (Laruelle, 2000). Future studies are required to replicate these observations with larger sample sizes.

Despite following the ROI segmentation guidelines of Tziortzi and colleagues (Tziortzi *et al*, 2011), we were unable to reliably estimate [^{11}C]-(+)-PHNO BP_{ND} in the ventral pallidum and hypothalamus in all our subjects. Despite this, we observed an increase in [^{11}C]-(+)-PHNO BP_{ND} in both of these D_3R-rich regions. Thus, while estimates of endogenous dopamine levels in D_3R-rich regions may be achieved with [^{11}C]-(+)-PHNO, these estimates could not be achieved in the hypothalamus and VP for all subjects due to poor SRTM model fitting associated with noise in the time activity curve and no washout of the signal. With our experience with [^{11}C]-(+)-PHNO, our group has noted the reliability of fitting in these regions is less than for the other ROIs. Thus, this may have contributed to the low statistical significance of the AMPT effect despite a high average change in BP_{ND}. However, it is reassuring that our reported BP_{ND} values for these regions are in accordance with the reports of other studies (Tziortzi *et al*, 2011). Moreover, we may have been underpowered to detect significant changes in these regions, given their reliability of fitting. Notably, no study has ever published test-retest reliability data for the hypothalamus and VP ROIs with [^{11}C]-(+)-PHNO. While this poses a limitation to our current investigation, it does not detract from the fact that after AMPT large average increases in BP_{ND} were observed in these ROIs. Future studies would benefit from reporting test-retest reliability of fitting for these ROIs.

Consistent with previous reports (Verhoeff *et al*, 2003), AMPT significantly decreased self-reported vigor and increased self-reported fatigue in healthy participants. Interestingly, the change in vigor scores under dopamine depletion was related to the change in [^{11}C]-(+)-PHNO BP_{ND} in the globus pallidus. Several case studies have reported that unilateral or bilateral lesions

to the globus pallidus, in particular the internal segment, can result in profound apathy and lack of motivation (Adam *et al*, 2013; Singh *et al*; Vijayaraghavan *et al*, 2008). It has also been demonstrated that D_3R are more abundant in the internal segment of the globus pallidus than D_2R (Gurevich and Joyce, 1999). Thus, we speculate that the significant decrease in vigor and motivation seen in participants after dopamine depletion may be mediated by reduced dopaminergic signaling at D_3R in the globus pallidus, as captured by the change in [^{11}C]-(+)-PHNO BP_{ND}.

There are several limitations with the current investigation worth addressing. First, our study was only single-blind and not placebo controlled, a limitation shared by all previous dopamine PET studies using AMPT. Secondly, we have not collected arterial plasma data, quantifying BP_{ND} using the simplified reference tissue method rather than using full-kinetic modelling. The simplified reference tissue method approach to estimate BP_{ND} with the cerebellum as reference has a good correlation with the BP as estimated with a full kinetic analysis and it was validated in controls for [^{11}C]-(+)-PHNO (Ginovart *et al*, 2007). The full kinetic analysis would allow direct estimation of the BP in the regions of interest without the potential bias induced by specific binding in the reference region, if any. Simply, we cannot rule out (quantitatively) that AMPT did not exert an effect in the reference tissue, and poses as a current limitation to our study. Finally, it has been noted that the injected mass of [^{11}C]-(+)-PHNO was not within ideal radiotracer conditions (i.e. <1.5 ng/kg) and consequently could lead to an underestimation of the occupancy by endogenous dopamine [see appendix in(Shotbolt *et al*, 2012)]. Unfortunately the specific activity required to obtain tracer conditions is not possible with the available radiosynthesis method. We do not believe this unavoidable technical limitation substantially changes the conclusion of our study. Since the radiotracer mass injected was similar

in both PET scan sessions, we are underestimating the apparent occupancy of the competitor dopamine by a similar factor in both scans. Furthermore, the PET scans were performed more than 24 hours apart avoiding any carry-over effect.

In conclusion, the current investigation is the first to estimate endogenous dopamine levels at D_2R and D_3R in healthy humans using the agonist radiotracer [^{11}C]-(+)-PHNO. [^{11}C]-(+)-PHNO is sensitive to acute dopamine depletion in humans, and future studies employing this radiotracer to estimate endogenous dopamine levels at D_2R and D_3R in neuropsychiatric populations are warranted.

Funding and Disclosure

This study was funded by Canadian Institutes of Health Research (MOP-114989) and U.S. National Institute of Health (RO1MH084886-01A2). Dr. Nakajima reports having received grants from Japan Society for the Promotion of Science and Inokashira Hospital Research Fund and speaker's honoraria from GlaxoSmith Kline, Janssen Pharmaceutical, Pfizer, and Yoshitomiyakuhin within the past 3 years. Dr. Graff-Guerrerro currently receives research support from the following external funding agencies: Canadian Institutes of Health Research, the U.S. National Institute of Health, and the Mexico Instituto de Ciencia y Tecnologıa para la Capital del Conocimiento en el Distrito Federal (ICyTDF). He has also received professional services compensation from Abbott Laboratories, Gedeon-Richter Plc, and Lundbeck; grant support from Janssen; and speaker compensation from Eli Lilly. Dr. Remington has received research support from the Canadian Diabetes Association, the Canadian Institutes of Health Research, Medicure, Neurocrine Biosciences, Novartis, Research Hospital Fund–Canada Foundation for Innovation, and the Schizophrenia Society of Ontario and has served as a consultant or speaker for Novartis, LaboratoriosFarmacéuticosRovi, Synchroneuron, and Roche. Mr. Caravaggio, Ms. Carol Borlido, Dr. Gerretsen, Dr. Sylvain Houle, and Dr. Wilson report no biomedical financial interests or potential conflicts of interest relevant to the current study.

Acknowledgements

The authors gratefully acknowledge Dr. Isabelle Bolieau for her insights and disclosing data. The authors thank the PET Centre staff at the Centre for Addiction and Mental Health, including Alvina Ng and Laura Nguyen, for technical assistance in data collection. They also thank Ms. Wanna Mar, Ms. Kathryn Kalahani-Bargis, and Ms. Zhe Feng for their assistance in participant recruitment.

References

Abi-Dargham A, Rodenhiser J, Printz D, Zea-Ponce Y, Gil R, Kegeles LS, *et al* (2000). Increased baseline occupancy of D2 receptors by dopamine in schizophrenia. *Proc Natl Acad Sci U S A* **97**(14): 8104-8109.

Abi-Dargham A, van de Giessen E, Slifstein M, Kegeles LS, Laruelle M (2009). Baseline and amphetamine-stimulated dopamine activity are related in drug-naive schizophrenic subjects. *Biol Psychiatry* **65**(12): 1091-1093.

Adam R, Leff A, Sinha N, Turner C, Bays P, Draganski B, *et al* (2013). Dopamine reverses reward insensitivity in apathy following globus pallidus lesions. *Cortex* **49**(5): 1292-1303.

Adolfsson R, Gottfries CG, Roos BE, Winblad B (1979). Post-mortem distribution of dopamine and homovanillic acid in human brain, variations related to age, and a review of the literature. *J Neural Transm* **45**(2): 81-105.

Banerjee A, Prante O (2012). Subtype-selective dopamine receptor radioligands for PET imaging: current status and recent developments. *Curr Med Chem* **19**(23): 3957-3966.

Bloemen OJ, de Koning MB, Gleich T, Meijer J, de Haan L, Linszen DH, *et al* (2013). Striatal dopamine D2/3 receptor binding following dopamine depletion in subjects at Ultra High Risk for psychosis. *Eur Neuropsychopharmacol* **23**(2): 126-132.

Cumming P (2011). Absolute abundances and affinity states of dopamine receptors in mammalian brain: A review. *Synapse* **65**(9): 892-909.

Cumming P, Wong DF, Dannals RF, Gillings N, Hilton J, Scheffel U, *et al* (2002). The competition between endogenous dopamine and radioligands for specific binding to dopamine receptors. *Ann N Y Acad Sci* **965**: 440-450.

Engelman K, Jequier E, Udenfriend S, Sjoerdsma A (1968). Metabolism of alpha-methyltyrosine in man: relationship to its potency as an inhibitor of catecholamine biosynthesis. *J Clin Invest* **47**(3): 568-576.

Freedman SB, Patel S, Marwood R, Emms F, Seabrook GR, Knowles MR, *et al* (1994). Expression and pharmacological characterization of the human D3 dopamine receptor. *J Pharmacol Exp Ther* **268**(1): 417-426.

Galineau L, Wilson AA, Garcia A, Houle S, Kapur S, Ginovart N (2006). In vivo characterization of the pharmacokinetics and pharmacological properties of [11C]-(+)-PHNO in rats using an intracerebral beta-sensitive system. *Synapse* **60**(2): 172-183.

Gallezot JD, Beaver JD, Gunn RN, Nabulsi N, Weinzimmer D, Singhal T, *et al* (2012). Affinity and selectivity of [(1)(1)C]-(+)-PHNO for the D3 and D2 receptors in the rhesus monkey brain in vivo. *Synapse* **66**(6): 489-500.

Ginovart N, Galineau L, Willeit M, Mizrahi R, Bloomfield PM, Seeman P, *et al* (2006). Binding characteristics and sensitivity to endogenous dopamine of [11C]-(+)-PHNO, a new agonist radiotracer for imaging the high-affinity state of D2 receptors in vivo using positron emission tomography. *J Neurochem* **97**(4): 1089-1103.

Ginovart N, Willeit M, Rusjan P, Graff A, Bloomfield PM, Houle S, *et al* (2007). Positron emission tomography quantification of [11C]-(+)-PHNO binding in the human brain. *J Cereb Blood Flow Metab* **27**(4): 857-871.

Gjedde A, Wong DF, Rosa-Neto P, Cumming P (2005). Mapping neuroreceptors at work: on the definition and interpretation of binding potentials after 20 years of progress. *Int Rev Neurobiol* **63**: 1-20.

Graff-Guerrero A, Redden L, Abi-Saab W, Katz DA, Houle S, Barsoum P, *et al* (2010). Blockade of [11C](+)-PHNO binding in human subjects by the dopamine D3 receptor antagonist ABT-925. *Int J Neuropsychopharmacol* **13**(3): 273-287.

Graff-Guerrero A, Willeit M, Ginovart N, Mamo D, Mizrahi R, Rusjan P, *et al* (2008). Brain region binding of the D2/3 agonist [11C]-(+)-PHNO and the D2/3 antagonist [11C]raclopride in healthy humans. *Hum Brain Mapp* **29**(4): 400-410.

Gunn RN, Lammertsma AA, Hume SP, Cunningham VJ (1997). Parametric imaging of ligand-receptor binding in PET using a simplified reference region model. *Neuroimage* **6**(4): 279-287.

Gurevich EV, Joyce JN (1999). Distribution of dopamine D3 receptor expressing neurons in the human forebrain: comparison with D2 receptor expressing neurons. *Neuropsychopharmacology* **20**(1): 60-80.

Innis RB, Cunningham VJ, Delforge J, Fujita M, Gjedde A, Gunn RN, *et al* (2007). Consensus nomenclature for in vivo imaging of reversibly binding radioligands. *J Cereb Blood Flow Metab* **27**(9): 1533-1539.

Kegeles LS, Abi-Dargham A, Frankle WG, Gil R, Cooper TB, Slifstein M, *et al* (2010). Increased synaptic dopamine function in associative regions of the striatum in schizophrenia. *Arch Gen Psychiatry* **67**(3): 231-239.

Kiss B, Horti F, Bobok A (2011). In vitro and in vivo comparison of [(3)H](+)-PHNO and [(3)H]raclopride binding to rat striatum and lobes 9 and 10 of the cerebellum: a method to distinguish dopamine D(3) from D(2) receptor sites. *Synapse* **65**(6): 467-478.

Lammertsma AA, Hume SP (1996). Simplified reference tissue model for PET receptor studies. *Neuroimage* **4**(3 Pt 1): 153-158.

Laruelle M (2000). Imaging synaptic neurotransmission with in vivo binding competition techniques: a critical review. *J Cereb Blood Flow Metab* **20**(3): 423-451.

Laruelle M, D'Souza CD, Baldwin RM, Abi-Dargham A, Kanes SJ, Fingado CL, *et al* (1997). Imaging D2 receptor occupancy by endogenous dopamine in humans. *Neuropsychopharmacology* **17**(3): 162-174.

Martinez D, Greene K, Broft A, Kumar D, Liu F, Narendran R, *et al* (2009). Lower level of endogenous dopamine in patients with cocaine dependence: findings from PET imaging of D(2)/D(3) receptors following acute dopamine depletion. *Am J Psychiatry* **166**(10): 1170-1177.

Mawlawi O, Martinez D, Slifstein M, Broft A, Chatterjee R, Hwang DR, *et al* (2001). Imaging human mesolimbic dopamine transmission with positron emission tomography: I. Accuracy and precision of D(2) receptor parameter measurements in ventral striatum. *J Cereb Blood Flow Metab* **21**(9): 1034-1057.

McCormick PN, Ginovart N, Wilson AA (2011). Isoflurane anaesthesia differentially affects the amphetamine sensitivity of agonist and antagonist D2/D3 positron emission tomography radiotracers: implications for in vivo imaging of dopamine release. *Mol Imaging Biol* **13**(4): 737-746.

Narendran R, Slifstein M, Guillin O, Hwang Y, Hwang DR, Scher E, *et al* (2006). Dopamine (D2/3) receptor agonist positron emission tomography radiotracer [11C]-(+)-PHNO is a D3 receptor preferring agonist in vivo. *Synapse* **60**(7): 485-495.

Newberg AB, Moss AS, Monti DA, Alavi A (2011). Positron emission tomography in psychiatric disorders. *Ann N Y Acad Sci* **25**(10): 1749-6632.

Rabiner EA, Slifstein M, Nobrega J, Plisson C, Huiban M, Raymond R, *et al* (2009). In vivo quantification of regional dopamine-D3 receptor binding potential of (+)-PHNO: Studies in non-human primates and transgenic mice. *Synapse* **63**(9): 782-793.

Searle G, Beaver JD, Comley RA, Bani M, Tziortzi A, Slifstein M, *et al* (2010). Imaging dopamine D3 receptors in the human brain with positron emission tomography, [11C]PHNO, and a selective D3 receptor antagonist. *Biol Psychiatry* **68**(4): 392-399.

Searle GE, Beaver JD, Tziortzi A, Comley RA, Bani M, Ghibellini G, *et al* (2013). Mathematical modelling of [(1)(1)C]-(+)-PHNO human competition studies. *Neuroimage* **68**: 119-132.

Seeman P (2013). Schizophrenia and dopamine receptors. *Eur Neuropsychopharmacol* **23**(9): 999-1009.

Seeman P, Ulpian C, Larsen RD, Anderson PS (1993). Dopamine receptors labelled by PHNO. *Synapse* **14**(4): 254-262.

Shotbolt P, Tziortzi AC, Searle GE, Colasanti A, van der Aart J, Abanades S, *et al* (2012). Within-subject comparison of [(11)C]-(+)-PHNO and [(11)C]raclopride sensitivity to acute amphetamine challenge in healthy humans. *J Cereb Blood Flow Metab* **32**(1): 127-136.

Singh A, Mahgoub N, Klimstra S *Apathy associated with a unilateral globus pallidus lesion: a case report* Int J Geriatr Psychiatry. 2011 Jul;26(7):765-6. doi: 10.1002/gps.2563.

Studholme C, Hill DL, Hawkes DJ (1997). Automated three-dimensional registration of magnetic resonance and positron emission tomography brain images by multiresolution optimization of voxel similarity measures. *Med Phys* **24**(1): 25-35.

Tatsch K, Poepperl G (2012). Quantitative approaches to dopaminergic brain imaging. *Q J Nucl Med Mol Imaging* **56**(1): 27-38.

Tziortzi AC, Searle GE, Tzimopoulou S, Salinas C, Beaver JD, Jenkinson M, *et al* (2011). Imaging dopamine receptors in humans with [11C]-(+)-PHNO: dissection of D3 signal and anatomy. *Neuroimage* **54**(1): 264-277.

Udenfriend S, Zaltzman-Nirenberg P, Nagatsu T (1965). Inhibitors of purified beef adrenal tyrosine hydroxylase. *Biochem Pharmacol* **14**(5): 837-845.

van Wieringen JP, Booij J, Shalgunov V, Elsinga P, Michel MC (2013). Agonist high- and low-affinity states of dopamine D(2) receptors: methods of detection and clinical implications. *Naunyn Schmiedebergs Arch Pharmacol* **386**(2): 135-154.

Verhoeff NP, Christensen BK, Hussey D, Lee M, Papatheodorou G, Kopala L, *et al* (2003). Effects of catecholamine depletion on D2 receptor binding, mood, and attentiveness in humans: a replication study. *Pharmacol Biochem Behav* **74**(2): 425-432.

Verhoeff NP, Hussey D, Lee M, Tauscher J, Papatheodorou G, Wilson AA, *et al* (2002). Dopamine depletion results in increased neostriatal D(2), but not D(1), receptor binding in humans. *Mol Psychiatry* **7**(3): 322-328.

Verhoeff NP, Kapur S, Hussey D, Lee M, Christensen B, Psych C, *et al* (2001). A simple method to measure baseline occupancy of neostriatal dopamine D2 receptors by dopamine in vivo in healthy subjects. *Neuropsychopharmacology* **25**(2): 213-223.

Versteeg DH, Van Der Gugten J, De Jong W, Palkovits M (1976). Regional concentrations of noradrenaline and dopamine in rat brain. *Brain Res* **113**(3): 563-574.

Vijayaraghavan L, Vaidya JG, Humphreys CT, Beglinger LJ, Paradiso S (2008). Emotional and motivational changes after bilateral lesions of the globus pallidus. *Neuropsychology* **22**(3): 412-418.

Willeit M, Ginovart N, Graff A, Rusjan P, Vitcu I, Houle S, *et al* (2008). First human evidence of d-amphetamine induced displacement of a D2/3 agonist radioligand: A [11C]-(+)-PHNO positron emission tomography study. *Neuropsychopharmacology* **33**(2): 279-289.

Wilson AA, Garcia A, Jin L, Houle S (2000). Radiotracer synthesis from [(11)C]-iodomethane: a remarkably simple captive solvent method. *Nucl Med Biol* **27**(6): 529-532.

Wilson AA, McCormick P, Kapur S, Willeit M, Garcia A, Hussey D, *et al* (2005). Radiosynthesis and evaluation of [11C]-(+)-4-propyl-3,4,4a,5,6,10b-hexahydro-2H-naphtho[1,2-b][1,4]oxazin-9-ol as a potential radiotracer for in vivo imaging of the dopamine D2 high-affinity state with positron emission tomography. *J Med Chem* **48**(12): 4153-4160.

Tables/Figure Legends

Table 1. Effect of alpha-methyl-para-tyrosine (AMPT) on various plasma levels (*n*=10).

Data are given as mean and standard deviation in parenthesis.

Table 2. Effect of alpha-methyl-para-tyrosine (AMPT) on self-report measures (*n*=10).

Data are given as mean raw scores with standard deviation in parenthesis.

*Denotes significance after FDR correction

Figure 1. [^{11}C]-(+)-PHNO BP_{ND} in each ROI before and after AMPT induced dopamine depletion.

Figure 2. Averaged [^{11}C]-(+)-PHNO voxel-wise BP_{ND} map of all subjects (*n*=10) before and after AMPT induced dopamine depletion.

Figure 3. Correlation between percent change in self-reported vigor and [^{11}C]-(+)-PHNO BP_{ND} in the globus pallidus.

Supplemental Table 1. [^{11}C]-(+)-PHNO BP_{ND} in each ROI before and after AMPT.

Data are given as mean raw scores with standard deviation in parenthesis.
$\%\Delta BP_{ND}$ was calculated as 100*((Depletion BP_{ND}-Baseline BP_{ND})/Baseline BP_{ND}

Supplemental Table 2. [^{11}C]-(+)-PHNO BP_{ND} for each subject before and after AMPT.

$\%\Delta BP_{ND}$ was calculated as 100*((Depletion BP_{ND}-Baseline BP_{ND})/Baseline BP_{ND}

Supplemental Figure 1. Averaged standardized uptake values of [^{11}C]-(+)-PHNO in each ROI before and after AMPT induced dopamine depletion.

Supplemental Text. Regulation of dopamine, and changes in [^{11}C]-(+)-PHNO BP_{ND} in response to dopamine challenges, in the substantia nigra.

Table 1. Effect of alpha-methyl-para-tyrosine (AMPT) on various plasma levels (*n*=10).

Plasma levels	Baseline	AMPT 5h	AMPT 27h	%Δ Over 27h	*P* value
Homovanillic Acid (HVA)					
nmol/L	81.8 (42.8)	37.0 (15.0)	32.4 (27.2)	-60%	0.009
3-Methoxy-4-hydroxphenyglycol (MHPG)					
nmol/L	188.3 (99.2)	160.5 (89.2)	109.5 (60.3)	-42%	0.0003
Alpha-methyl-prara-tyrosine (AMPT)					
umol/L		63.1 (38.2)	123.0 (53.0)	+95%	0.009

Data are given as mean and standard deviation in parenthesis.

Table 2. Effect of alpha-methyl-para-tyrosine (AMPT) on self-report measures (*n*=10)

Scales	Baseline Scores	AMPT 5h Scores	AMPT 27h Scores	%ΔScores Over 27h	*P* value	FDR *P* Threshold
Profile of Mood States (POMS)						
Fatigue	9.6 (3.6)	10.4 (3.7)	15.4 (6. 1)	+66.4%	0.0068*	0.008
Vigor	25.7 (9.2)	23.4 (5.9)	19.4 (7.1)	-21.8%	0.0046*	0.017
Tension	11.1 (2.3)	11.9 (3.3)	13 (4.5)	+15.5%	0.0463	0.025
Depression	16.3 (3.1)	16.0 (3.1)	18.9 (7.9)	+13.4%	0.1817	0.033
Confusion	11.9 (2.1)	11.7 (2.3)	13.3 (4.7)	+11.6%	0.2606	0.042
Anger	12.5 (1.1)	13 (2.0)	13.8 (4.8)	+9.3%	0.3464	0.050
Subjective well-being under neuroleptic treatment (SWN)						
Physical Functioning	22.2 (1.5)	22 (1.6)	19.9 (2.8)	-10.5%	0.0094	0.007
Negative Sum	57.7 (2.3)	56.9 (3.0)	54.2 (4.4)	-6.10%	0.0105*	0.014
Emotion Regulation	22.4 (1.3)	21.8 (1.8)	21 (2.5)	-6.36%	0.0498	0.021
Mental Functioning	22 (1.6)	21.7 (2.1)	20.3 (3.2)	-7.91%	0.0523	0.029
Positive Sum	52.6 (5.5)	51.5 (6.1)	48.3 (10.8)	-8.88%	0.0867	0.036
Self-control	22.3 (1.4)	22.2 (1.4)	20.9 (3.8)	-6.58%	0.1914	0.043
Social Integration	21.4 (2)	20.7 (2.4)	20.4 (3.2)	-4.71%	0.2289	0.050

Data are given as mean raw scores with standard deviation in parenthesis.

*Denotes significance after FDR correction

A

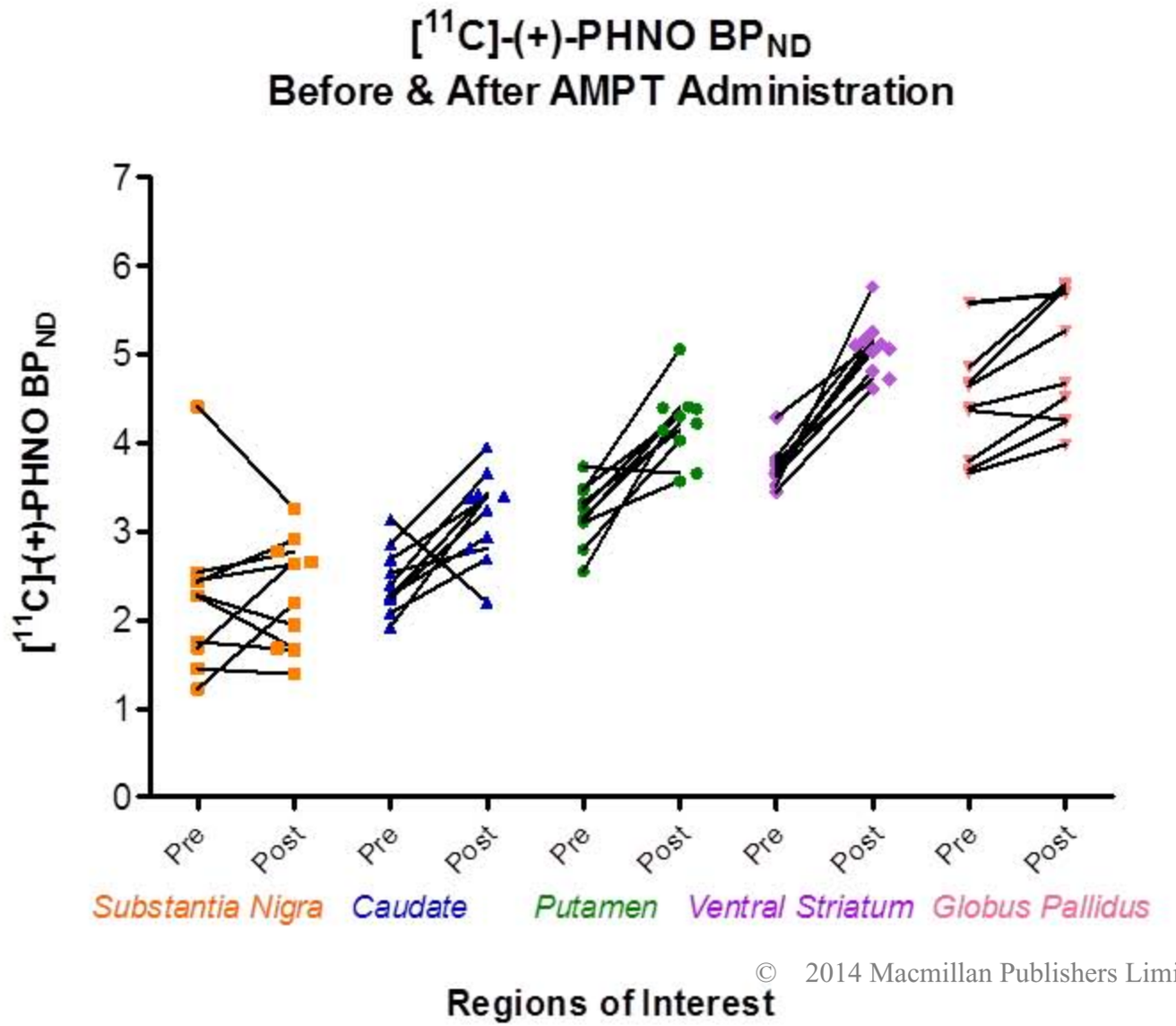

B